THE GEMINI DEEP DEEP SURVEY:

Status Report and Overview of the GMOS Nod-and-Shuffle Mode

The Gemini Deep Deep Survey Team

R. G. Abraham (University of Toronto; Canadian Principal Investigator); K. Glazebrook (Johns Hopkins University; Co-U.S. Principal Investigator); P. McCarthy (Observatories of the Carnegie Institution of Washington; Co-US Principal Investigator); R. Carlberg (University of Toronto); H. W. Chen (Massachusetts Institute of Technology); D. Crampton (Herzberg Institute of Astrophysics, National Research Council [NRC] Canada); I. Hook (Oxford University); I. Jørgensen (Gemini Observatory) R. Marzke (San Francisco State University); R. Murowinski (Herzberg Institute of Astrophysics, NRC Canada); K. Roth (Gemini Observatory); S. Savaglio (Johns Hopkins University)

Conventional spectroscopy of galaxies at redshifts of 1<z<2 suffers from technical challenges and the lack of strong spectral features at visible wavelengths. To date, near-infrared spectroscopy has yielded results for only a handful of high-star-formation-rate objects, and the multiplexing advantages of multi-aperture near-infrared spectrographs are modest at best. In principle, redshifts and diagnostic spectra can be obtained over 1<z<2 via ultradeep, poisson-limited spectroscopy on 8-meter-class telescopes, by targeting weak absorption features in the rest ultraviolet spectra of galaxies. However, unless exposure times are short (less than a few hours), Multi-Object Spectrograph (MOS) spectroscopy with 8-meter-class telescopes is generally not photon-limited. The main contributors to the noise budget are imperfect sky subtraction and fringe removal. The product of these difficulties is the so-called redshift desert, a paucity of optical redshifts at 1<z<2.

The position in redshift space of this redshift desert is a major problem for studies of galaxy evolution because it seems to span the major epoch of galaxy building. Intermediate-redshift surveys e.g., *Canada-France Redshift Survey (CFRS;* Lilly, et al., 1995) reveal that 50 to 100 percent of the stellar mass in L>L* galaxies was in place by z=1. At higher redshifts, the Lyman Break galaxies contain approximately (~) 20 percent of the present-day stellar mass (Shapley, et al., 2001). Therefore, the redshift range over which most of the mass is being built up in galaxies is exactly the range in which spectroscopic redshifts are notoriously difficult to obtain.

One way forward out of this dilemma is to use an innovative new approach to sky subtraction and multiplexing known as "nod and shuffle" (Glazebrook & Bland-Hawthorn, 2001; Cuillandre, et al., 1994). "Nod and shuffle" (N&S) is a mode of observing where parts of the charge-coupled device (CCD) are used as a "storage register" in a beam-switched image. Beam-switching is achieved by rapid alternation between object and sky positions ("nodding"), which is undertaken with no readout penalty. Instead, the sky image is shuffled to a storage region. Typically, nodding takes place every 30–60 seconds, which is a timescale faster than the variations of airglow emission lines. Because both the sky and objects are observed quasi-simultaneously through the same optical path, slits and pixels, N&S provides an order of magnitude improvement in sky subtraction opening up significant new observational capabilities for large telescopes. For example, very deep integrations (ten times longer than is practical with conventional spectroscopy) are possible with N&S at very high slit densities.

GMOS Nod and Shuffle

In the last 12 months, our team proposed, developed and commissioned a nod-and-shuffle mode for the Gemini Multi-Object Spectrograph (GMOS) in order to undertake the *Gemini Deep Deep Survey (GDDS)*, the deepest redshift survey ever undertaken. This work was performed using the Frederick C. Gillett Gemini Telescope (Gemini North) on Mauna Kea, Hawai'i. The resources for this effort were provided by a unique university-institutional partnership bringing together the Gemini Observatory, the Herzberg Institute of Astrophysics (HIA), the National Optical Astronomy Observatory (NOAO), Carnegie Observatories, Johns Hopkins University and the University of Toronto. Early results from our survey will be shown at the end of this article, and all data from the GDDS will be made publicly available soon at the project website (http://www.ociw.edu/lcirs/gdds.html).

Nod and shuffle is now a fully supported common-user mode for GMOS. The GMOS implementation of the mode represents a significant technical advance in two ways: (1) this is the first time N&S has been implemented on an 8-meter-class facility, and (2) this is the first time N&S has been used to shuffle multiple CCDs (the three GMOS EEVs, simultaneously).

Since this mode will be of interest to many readers of this newsletter who are not followers of recent developments in faint galaxy evolution, we briefly digress from our survey to describe the basic nod-and-shuffle concept and its specific implementation on GMOS before describing the early results from the GDDS in the next section. Readers interested in the details of GMOS N&S at a level beyond that which we have space for here are referred to the following web page: http://www.gemini.edu/sciops/instruments/gmos/gmosIndex.html.

It is important to emphasize that in most ways N&S observing with GMOS is the same as normal observing with the instrument. However, life is far simpler with N&S mode once the photons have been collected because sky subtraction is reduced to a trivial operation e.g., a single Image Reduction and Analysis Facility (IRAF) command that subtracts the skies as an entire frame of data in one step automatically. As will be described below, the added complexity of N&S comes at the initial mask design stage.

The observing procedure for N&S is as follows:

1) Calibration data (arcs/flats/standards/ etc.) are obtained in the normal way. It is not necessary to shuffle these. In fact, it may not even be necessary to use them to first order N&S as it makes bias and flat field corrections unnecessary. For higher order corrections, it may be necessary to shuffle bias/dark frames. If biases and darks are to be taken in N&S mode, then for bias frames the number of nod and shuffle cycles (described below) should be the same as for the science observations. For dark frames, all parameters should be identical to those for the science observations.

2) The field should be acquired in the normal way by centering the reference stars in their mask apertures.

3) Guide stars should be set up on probes, and their placement should bear in mind the nod vector.

At this point several parameters must be set before N&S observations can be initiated. These are: (i) the shuffle distance, Y; (ii) the subintegration time; and (iii) the number of subintegrations. With the specification of these parameters, the N&S observation can be initiated. The observing system proceeds by activating the following nod-and-shuffle sequence:

1) An observation is taken at a first position on the sky (position A) while guiding.

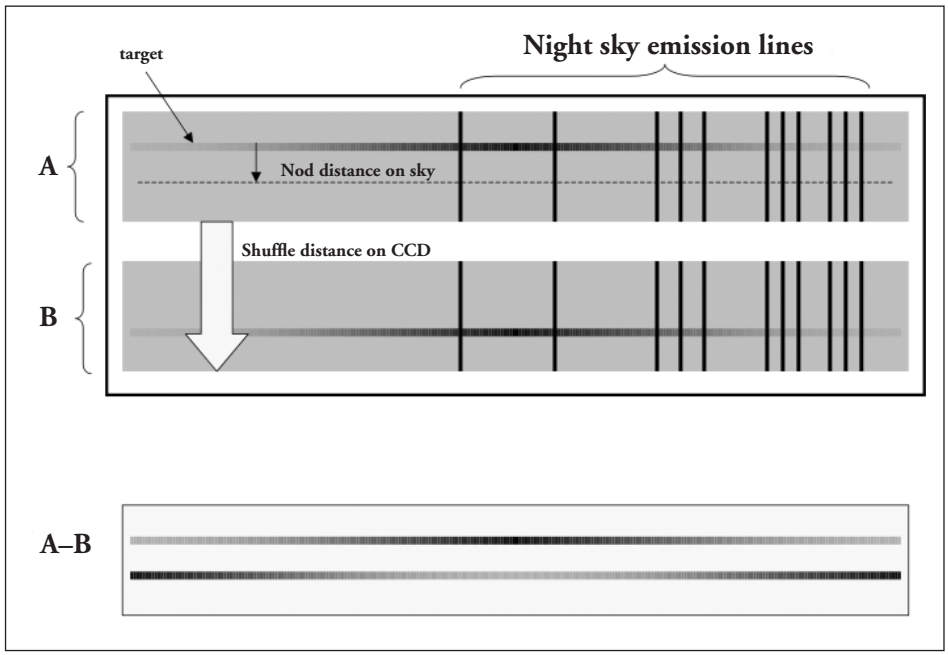

Figure 1: *Schematic of nod-and-shuffle for a single slit. When the telescope is in the "object" position, CCD area "A" records a spectrum. The "sky" position records the nodded spectrum (in this case the telescope has been nodded a few arcseconds along the slit direction). The area "B" is non-illuminated by the mask and serves as a storage area for the "sky position." The image difference subtracts the sky, and leaves a positive and negative object spectrum for subsequent extraction.*

2) The shutter is closed, and charge is shuffled by +Y pixels.

3) The telescope is moved to a second position (position B).

4) The shutter is opened at position B, and the observation is continued.

5) The shutter is closed, and charge is shuffled by -Y pixels.

6) The telescope is moved back to position A.

7) The procedure is iterated until the exposure is complete. The final exposure time is the product of the subintegration time and the number of subintegrations.

In addition to these steps, we have found that (because of low-level charge traps in the EEV detectors) the quality of combined N&S spectra is enhanced by dithering the GMOS detector controller translation stage and central wavelength position slightly between long exposures.

The common case of nodding along a slit is shown schematically in ***Figure 1*** for a single slit. The close coordination required between telescope motion and charge motion embodied by this sequence is fully automated. Once initiated, it is transparent to the observer at the telescope. All that is required to subtract the sky from the spectrum is to subtract the sky portion of the CCD image from the object portion of the CCD image (conveniently accomplished with the *gnssky* subtask in the Gemini IRAF software distribution). At this point, the sky-subtracted spectrum can be extracted in the usual way with the usual tools. As will be described below, some mask designs allow the object to be observed at a different position on the slit, or on a separate slit, while the telescope is at position B. In which case, a positive and negative object spectrum results, and the two must be extracted separately (and the latter needs to be multiplied by -1 before the two spectra added together can maximize the signal-to-noise ratio).

A trade-off between observing efficiency and multiplexing lies at the heart of N&S, and this can make mask design quite tricky. The optimal mask design depends sensitively on target brightness and sky density. For example, one may choose to maximize multiplexing using many

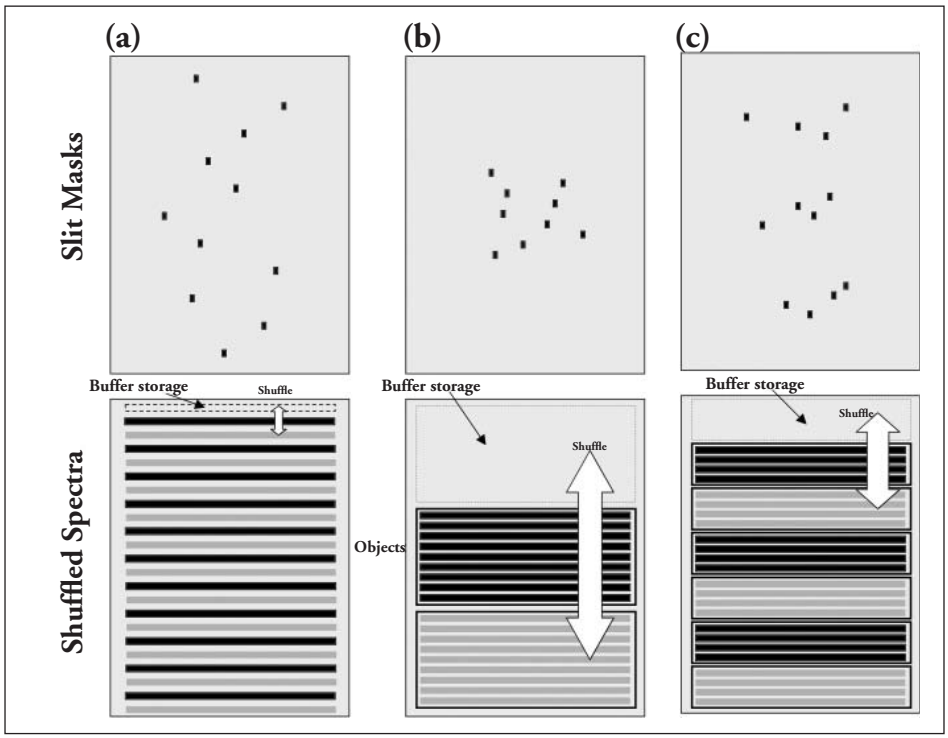

Figure 2: *Illustration of masks with different shuffle distances. The top row shows the input masks, and the bottom row shows the resulting shuffled object-sky spectra. The black spectra correspond to image A in Figure 2, and the light grey spectra correspond to image B in the same figure; (a) a mask where the shuffle is only a few pixels, and the sky is stored below the object – appropriate for extended, relatively low-source-density regions. (b) a mask where the shuffle is large, appropriate for cases with compact regions of high-source density. (c) an intermediate case. This compromise has the advantage of allowing a high-density extended field to be tacked while minimizing the number of object-storage interfaces where it is necessary to leave gaps. Note that in reality the area we have shown as a single "detector" is three CCDs (in GMOS, these are arranged left to right).*

small slits ("microslits"), or even holes, as an extended slit is not required for sky-subtraction. Alternatively, one may wish to maximize on-source integration time by observing the object in both the nominal "object" and "sky" positions in which case it is either necessary to have a long enough slit to accommodate the nod or to have a pair of holes. Some of the considerations and some suggestions for mask design are illustrated in ***Figure 2***. We illustrate two extreme cases as well as an intermediate case, which in many circumstances will be the best compromise:

Case 1 (***see Figure 2a***): The shuffle distance is small, and the sky image is recorded immediately below each object image. In this limit (for high densities), 50 percent of the detector is used for storage. The packing density is limited by the necessity to leave small gaps between the images to allow for the Point Spread Function (PSF) width. This case is perhaps the easiest to deal with as it requires no modification to the mask-making software. One can design effective masks by just pretending the effective slit length is bigger, and by nodding along the slit. This is a good mask design strategy if the density of the most interesting sources is sufficiently low.

Case 2 (***see Figure 2b***): The whole field is shuffled in one large shuffle. In this case, 66% of the detector must be used for storage, which is larger than ***Case 1***, but still less than standard MOS modes. This would be a good design for fields in which a compact distribution of objects is to be observed (such as a grouping of HII regions or emission-line knots in a single galaxy).

Case 3 (***see Figure 2c***): An intermediate case. In many cases, a design such as this is probably optimal in terms of packing density and minimization of storage overhead. Here the number of interfaces between object-sky regions in the mask is reduced since these have to be greater than the instrumental PSF width.

For the *GDDS*, we chose to use a ***Case 1*** mask design because our prime targets (infrared-selected candidate 1<z<2 galaxies) have a source density low enough (~50 to 100 objects/mask) that extreme multiplexing is not required.

Early Data From the Gemini Deep Deep Survey

The *GDDS* is a joint US-Canadian Band-1 Gemini redshift campaign targeting galaxies at 1<z<2. Four independent fields are being observed with GMOS for ~100,000 seconds each to a limiting magnitude of I(AB)=24.7. The

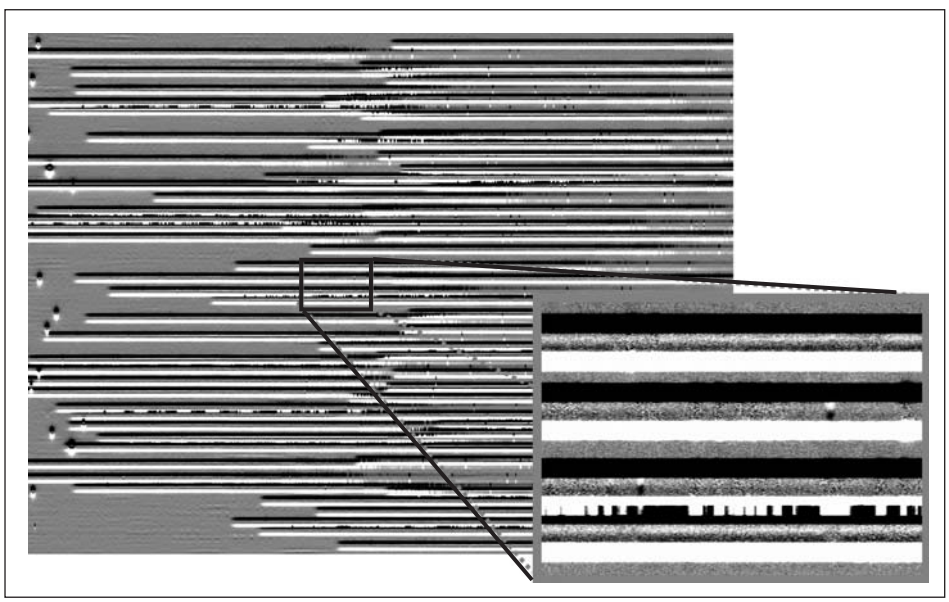

Figure 3: *An image showing the "supercombined" GDDS 22h mask. Object spectra are sandwiched between positive and negative sky spectra on the mask. The inset shows a blow-up of a small region showing part of four spectra. These show positive and negative continua and emission lines.*

microshuffling mode of N&S allows us to observe 65 to 85 red-selected galaxies in each 5'x5' GMOS field. Two fields have been completed to date, and the two remaining fields are being observed in semester 2003A.

Our sample is taken from the *Las Campanas Infrared Survey (LCIR)* and is K-band selected to a limit of K=20.8 that is nearly a magnitude deeper than the K20 survey (McCarthy, et al., 2001; Chen, et al., 2001; Firth, et al., 2001). Photometric redshifts from the 8-color LCIR imaging survey allow us to reject the z<1 foreground. The high-slit density afforded by N&S allows us to add additional I-band-selected and photo-z-filtered objects in regions of the field devoid of suitable K-selected objects. A sky-subtracted GMOS frame showing how this sky density is translated to spectral coverage on the CCD frame is shown in ***Figure 3***. This frame is the result of running a combined data frame through the Gemini IRAF package's *gnssky* subtask, which is used to subtract a shifted copy of the image from itself, resulting in regions of clean-sky-subtracted slits sandwiched between light and dark bands that correspond to noise where the data has been subtracted out-of-phase.

The *GDDS* is presently achieving >90 percent spectroscopic completeness and median spectroscopic redshifts of z=1.1 to 1.2 with essentially no contamination by galaxies at redshifts z<0.8 and a tail to z=2 in each field. The total *GDDS* sample will be comprised of ~300 galaxies with redshifts at 0.8<z<2.0. Approximately 150 of which are candidate early-type systems. Our focus is squarely upon the most massive systems at high redshifts. Unlike most high-redshift surveys, we are not biased in favor of selecting high-star-formation-rate systems. Around 40 percent of the redshifts in our sample are of pure absorption-line galaxies with no detectable (or at best very weak) emission features. Representative spectra from the *GDDS* are shown in ***Figure 4***. The first spectrum is of a post-starburst elliptical galaxy at z=1 that is near both

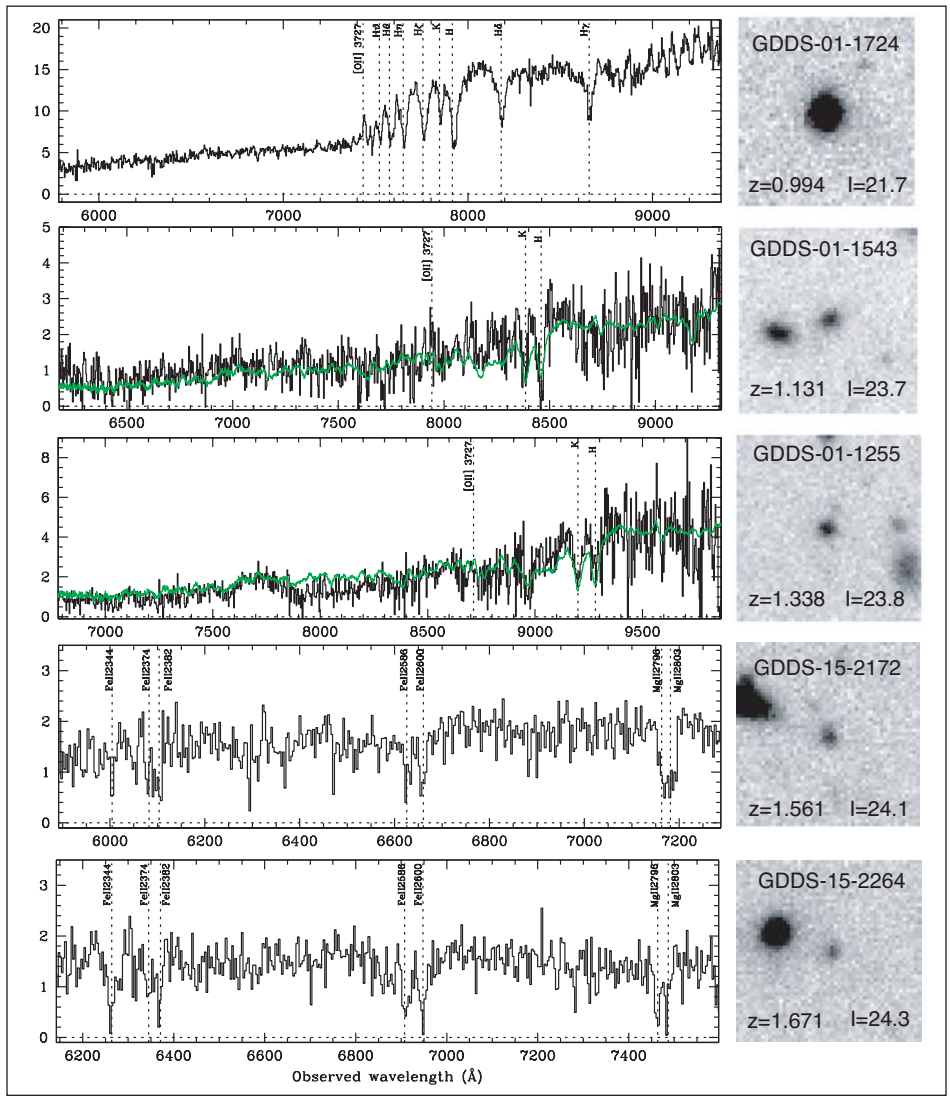

Figure 4: *Montage of 100ks Gemini GMOS nod-and-shuffled spectra from the GDDS. Ground-based I-band images (in ~0.8 arcsecond seeing) are shown at right. Objects shown span a redshift range of 0.994<z<1.671 and a magnitude range of 21.7<I<24.3 magnitude. A post-starburst system with prominent Balmer absorption features is shown at top followed by two quiescent early-type systems (with early-type spectral templates superimposed). About 40 percent of the red population shows similar spectra. The bottom two spectra show blue ultraviolet continua, consistent with recent star formation, together with narrow interstellar medium (ISM) absorption lines (MgII, FeII).*

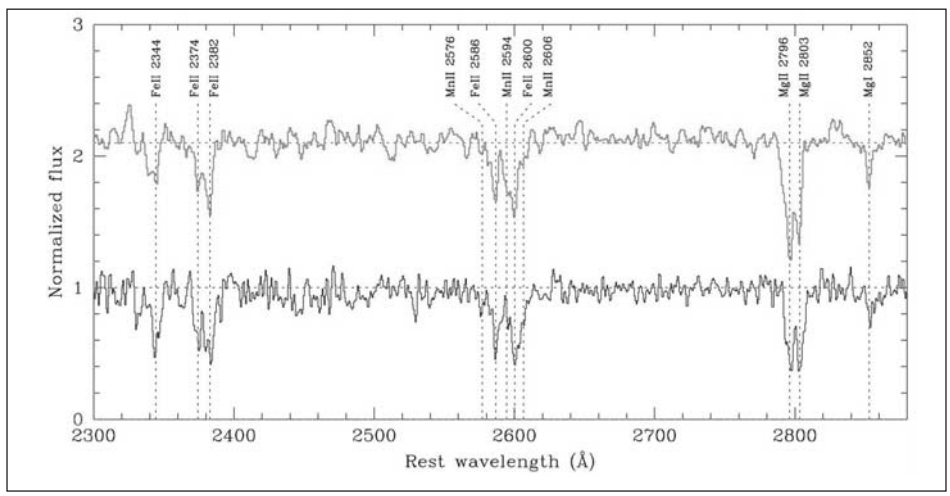

Figure 5: *Lower black curve: Composite GDDS spectrum of 13 galaxies with strong ISM absorption lines. The redshift range covered by the spectra is 1.260<z<1.895 (with a mean of z=1.53). This sample represents about 29 percent of the total number of galaxies detected by the first two masks of the GDDS in the redshift interval 1.13<z<2.00. Detected absorption features are marked by the dotted lines. As a reference, we also show the composite spectrum of 14 local starburst-dwarf galaxies observed with HST/FOS (upper gray curve). This spectrum has been magnified for comparison.*

the redshift and magnitude limit of the *CFRS*. This spectrum illustrates the spectacular signal-to-noise ratio achieved in 100ks with Gemini/GMOS for galaxies near the limits of the previous generation of surveys. Each of the four other representative spectra demonstrate our ability to determine absorption line redshifts squarely in the middle of the so-called redshift desert, and show canonical ultraviolet spectral features and the typical signal-to-noise achieved for fainter galaxies in our sample. GDDS-01-1543 (z=1.13) and GDDS-01-1255 (z=1.34) are well matched by a local early-type galaxy template (overlaid on the object spectra in the figure), while GDDS-15-2172 (z=1.56) and GDDS-15-2264 (z=1.67) show narrow metallic absorption features characteristic of local starbursts and originating in the galaxies' interstellar medium (ISM).

The K-band-selected objects in ***Figure 4*** that are red at rest visual wavelengths but which show blue rest-ultraviolet continua are particularly interesting. ***Figure 5*** shows a composite spectrum obtained by combining individual spectra for 13 such systems at 1.3<z<1.9. The resulting spectrum is quite comparable in signal-to-noise to a stack of 14 local dwarf-starburst spectra obtained with HST/FOS (kindly supplied by C. Tremonti) and also shown in the figure. The *GDDS* spectral database is of sufficiently high signal-to-noise to allow a myriad of uses aside from the basic goal of obtaining redshifts. The column density distribution implied by the narrow ISM lines in this figure will be the focus of one of the first *GDDS* papers (Savaglio, et al., 2003) prepared by our team.

A comparison between the colors and redshifts of GDDS galaxies and those of local samples and of Lyman Break galaxies from the Hubble Deep Field (HDF) is shown in ***Figure 6***. This figure illustrates the remarkable success of the *GDDS* in opening in probing the poorly understood 1<z<2-redshift range. More importantly, the figure also shows that the *GDDS* is opening up this redshift range in a manner that is unbiased with respect to star-formation rate. This is in sharp contrast to studies with strong star-formation rate-selection biases, such as infrared surveys targeting emission lines at similar redshifts to the *GDDS*, or Lyman Break selection at higher redshifts. The colors of Lyman Break galaxies in HDF are ~2 magnitudes bluer than our sample. Because of its depth and underlying infrared selection characteristics, the *GDDS* is at present the only redshift survey capable of constraining the space density of quiescent, evolved, massive early-type galaxies at the peak epoch of galaxy assembly.

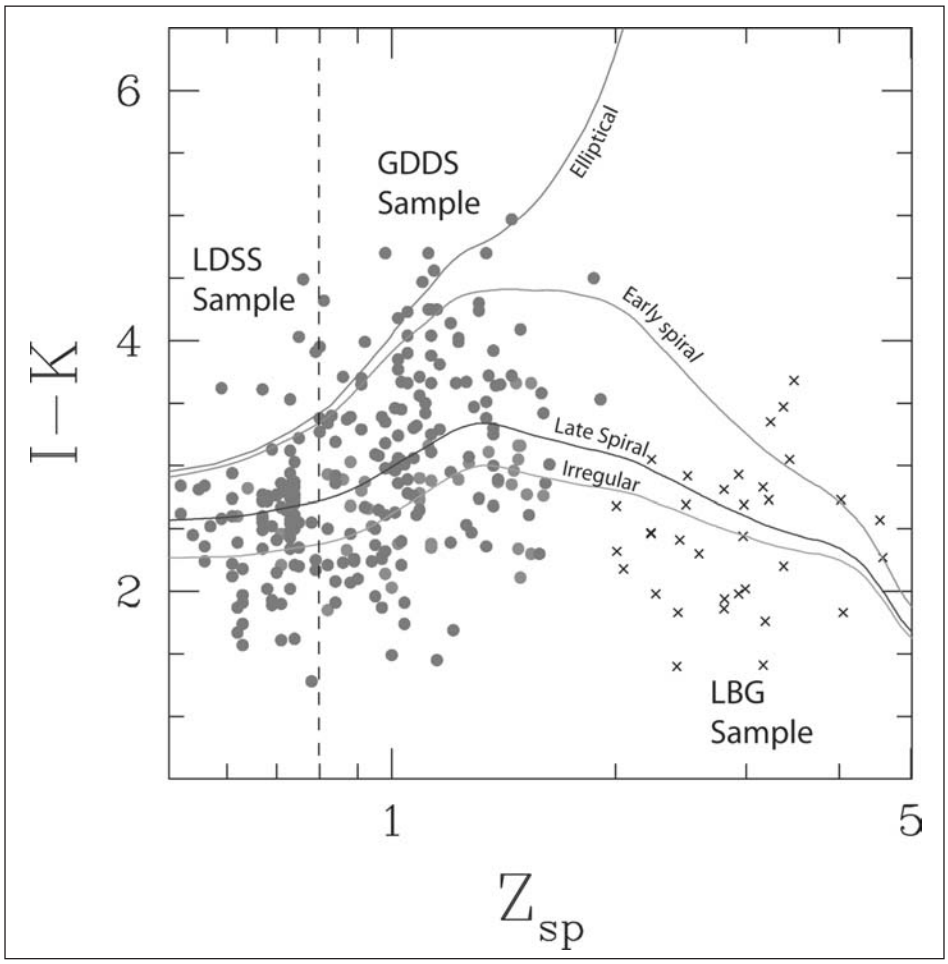

Figure 6: *I-K color as a function of redshift for the GDDS + LDSS (Low-Dispersion Survey Spectrograph) sample (solid circles) and for a sample of Lyman Break galaxies (crosses) in the HDF (courtesy of Mark Dickinson and collaborators). Note that the GDDS has few galaxies at z<0.8 (none at all in our latest mask), and the z<0.8 points shown come from LDSS spectroscopy of the GDDS fields we have undertaken with Magellan. Conversely, almost all points at z>0.8 are from the GDDS. Tracks correspond to the predictions of spectral synthesis models for a variety of star-formation histories. Note how the GDDS spans nearly the whole of the so-called redshift desert at 1<z<2, and is sensitive to the full range of possible star-formation histories, including quiescent early-type systems that may hold substantial mass yet remain undetectable in other surveys. Points shown in lighter gray are fainter than the K-band magnitude limit of the survey but were included to fill unused portions of our masks.*

REFERENCES:

Chen, H.W.; McCarthy, P. J.; & Marzke, R. O., et al., 2002, Ap.J., 570, 54.
Chen, H.W.; Marzke, R. O.; & McCarthy, P. J., et al., 2003, Ap.J., in press.
Cuillandre, J. C., et al., 1994, A&A, 281, 603.
Firth, A. E.; Somerville, R.; & McMahon, R. G, et al., 2002, MNRAS, 332, 617.
Glazebrook, K. & Bland-Hawthorn, J., 2001, PASP, 113, 197.
Lilly, S., et al., 1995, Ap.J, 455, 108.
McCarthy, P. J.; Carlberg, R. G.; Chen, H. W.; & Marzke, R. O., et al., 2001, Ap.J., 560, L131.
Shapley, A., et al., 2001, Ap.J., in press (astro-ph/01073234).
Steidel, et al., 1999, Ap.J., 519, 1.